Article

Studying the Association between Green Space Characteristics and Land Surface Temperature for Sustainable Urban Environments: An Analysis of Beijing and Islamabad

Shahid Naeem [1,2] (ID)**, Chunxiang Cao [1,2,*], Waqas Ahmed Qazi [3], Mehdi Zamani [1,2]** (ID)**, Chen Wei [1,2], Bipin Kumar Acharya [1,2]** (ID) **and Asid Ur Rehman [4]** (ID)

[1] State Key Laboratory of Remote Sensing Science, Institute of Remote Sensing and Digital Earth, Chinese Academy of Sciences, Beijing 100101, China; shahid@radi.ac.cn (S.N.); madiz@radi.ac.cn (M.Z.); chenwei@radi.ac.cn (C.W.); bipin@radi.ac.cn (B.K.A.)

[2] University of Chinese Academy of Science, Beijing 100049, China

[3] Institute of Space Technology, Islamabad 44000, Pakistan; waqas.qazi@grel.ist.edu.pk

[4] United Nations Human Settlements Program, Islamabad 44000, Pakistan; asid.rehman@gmail.com

* Correspondence: caocx@radi.ac.cn; Tel.: +86-139-1161-0226

Abstract: Increasing trends of urbanization lead to vegetation degradation in big cities and affect the urban thermal environment. This study investigated (1) the cooling effect of urban green space spatial patterns on Land Surface Temperature (LST); (2) how the surrounding environment influences the green space cool islands (GCI), and vice versa. The study was conducted in two Asian capitals: Beijing, China and Islamabad, Pakistan by utilizing Gaofen-1 (GF-1) and Landsat-8 satellite imagery. Pearson's correlation and normalized mutual information (NMI) were applied to investigate the relationship between green space characteristics and LST. Landscape metrics of green spaces including Percentage of Landscape (PLAND), Patch Density (PD), Edge Density (ED), and Landscape Shape Index (LSI) were selected to calculate the spatial patterns of green spaces, whereas GCI indicators were defined by Green Space Range (GR), Temperature Difference (TD), and Temperature Gradient (TG). The results indicate that both vegetation composition and configuration influence LST distributions; however, vegetation composition appeared to have a slightly greater effect. The cooling effect can be produced more effectively by increasing green space percentage, planting trees in large patches with equal distribution, and avoiding complex-shaped green spaces. The GCI principle indicates that LST can be decreased by increasing the green space area, increasing the water body fraction, or by decreasing the fraction of impervious surfaces. GCI can also be strengthened by decreasing the fraction of impervious surfaces and increasing the fraction of water body or vegetation in the surrounding environment. The cooling effect of vegetation and water could be explained based on their thermal properties. Beijing has already enacted the green-wedge initiative to increase the vegetation canopy. While designing the future urban layout of Islamabad, the construction of artificial lakes within the urban green spaces would also be beneficial, as is the case with Beijing.

Keywords: urban thermal environment; green space cool islands (GCIs); vegetation configuration; vegetation composition; GCI indicators; surface urban heat islands

1. Introduction

Consequent to the critical process of rapid urbanization, the contemporary structure and function of cities have been changing [1,2], through expansion of urban periphery, modification of ecological diversity, and energy flows [3–5]. Among proximate determinants, urban expansion or urban sprawl

primarily depends on socio-economic factors, migration from rural to urban areas, urban planning, and land use policies. [1,2,6–8]. Lack of landscape policies and inappropriate urban planning are rapidly increasing city sizes in developing countries. Consequently, the natural vegetation is being replaced by residential and commercial land. As a result, the surface temperature of urban regions is increasing more rapidly than its surroundings. The phenomenon of higher urban surface temperature is technically referred to as surface urban heat islands (SUHIs) [9,10]. This phenomenon is generally observed in cities, and its intensity depends on several factors including size, population, location, socio-economic activities, urban planning, and land use policies of the area under consideration [7,10–14].

SUHIs occur due to anthropogenic activities—especially urban development, which uses materials that can absorb thermal radiations effectively and raise the Land Surface Temperature (LST) of urban centers [15]. SUHIs are one of the key environmental issues of the 21st century [16]. The first research on SUHIs was reported in 1818, and since then it has become a very important research focus in urban ecology and urban climatology [17]. SUHI significantly defines the difference between urban surface temperature and its surroundings, which is ultimately associated with land use/land cover (LULC) changes and human energy use [18]. With the passage of time, the temperature difference between urban and rural areas is increasing. Consequently, vegetation covers and soil areas are being replaced by larger impervious surfaces and urban structures made of asphalt and concrete with various densities and heights [19,20]. Urban green spaces (UGSs) provide natural shade and absorb thermal radiation during the process of transpiration and photosynthesis, and help to mitigate the urban surface thermal impacts [21–23]. The goal of SUHI mitigation can be achieved by proper landscape planning. Therefore, this study on evaluation indices and impact factors is significantly valuable [24,25].

The modern concepts of remote sensing imagery are being applied broadly in SUHI studies. The basic idea behind the concept principle is to calculate LST from the satellite images and find the relationship with land cover classes. This method achieves good spatial coverage and synchronicity, which helps to overcome the flaws associated with conventional methods. The cooling effect of UGSs produce green space cool islands (GCIs), and have been proved in many studies using remotely-sensed imagery [26–28]. UGS refers to green infrastructure, including belts, urban parks, and residential green patches [29]. Plenty of research has already investigated the relationship between LST and GCIs, including landscape pattern, size and type of green space [12,28,30,31]. Cao et al. and Lu et al. [31,32] have exposed a nonlinear relationship between surface temperature and the green space area. Furthermore, when the area of a green space exceeds a certain threshold, its cooling effect drops sharply [33]. It has also been proved by Wong et al. and Jonsson et. al. [34,35] that the cooling effect of different vegetation types differs significantly; the highest cooling effect is provided by trees, and the lowest by shrubs and grasses.

Similarly, a number of previous investigations have also revealed that the composition and configuration of urban green spaces have a significant effect on surface temperature. For example, Li et al. [12] explored the relationship of green space configuration and composition with LST, and found a substantial negative correlation of green spaces with LST. Configuration refers to the distribution or spatial arrangement of land cover features [36]. In contrast, composition is the variety and abundance of land cover features, and does not consider their arrangements and other spatial characters [33,37]. These two elements also need to be studied comprehensively because it is not convenient to increase the amount of vegetation due to a lack of physical space within highly urbanized areas. In this situation, spatial arrangements of vegetation can help to minimize SUHI effects on urban landscapes [12,38–40]. Remarkable studies on the relationship between the composition of green spaces and LST over last two decades have consistently shown negative correlation, but magnitude varies among those reports. Configuration and other spatial characteristics of green spaces have a substantial effect on SUHI distribution within an urban environment [22,26,31,41]. Most of the literature has shown significant effects of green space shape and size on SUHI to produce urban cool islands [26,42]. Li et al. (2012) [12] studied the heavily urbanized metropolitan area of Beijing, and concluded that an

increase in patch density results in higher LST. This indicates that configuration plays an important role in LST variations.

Green space Range (GR), Temperature Gradient (TG), and Temperature Difference (TD) are the GCI features of green spaces, and are technically referred to as GCI indicators. TG and TD are not used frequently but have been used in a limited number of studies. Overall, the impact factors inside and outside of a green space include: landscape pattern, area, percentage of land cover types, and vegetation types. The information around the GCI has rarely been studied. Thus, it is important to study the relationship of these GCI indicators with impact factors inside and outside of the green spaces. Thus, one of the motives of the current work was to analyse relationship of these GCI indicators with impact factors inside and outside of green spaces. Percentage of Landscape (PLAND) was selected as a composition element, whereas Edge Density (ED), Patch Density (PD), and Landscape Shape Index (LSI) were selected as configuration elements.

This study was carried out in two capital cities: Beijing, China and Islamabad, Pakistan. Beijing is a heavily urbanized city and is expanding at a rapid rate compared to Islamabad. The present SUHI situation of Islamabad is better than Beijing's, but being a capital city of the country it is expected to expand rapidly and can face the same problems in future. Islamabad is a poorly studied area, and is still at an early growing stage. This research will help the urban planners to design appropriate city layout in the future by learning from the initiatives taken by the Chinese government for Beijing. In this study, the selected green space samples from densely urbanized regions of Beijing and Islamabad were analyzed by utilizing the high-resolution satellite imagery of Gaofen-1 (GF-1) and medium-resolution imagery of Landsat-8. The purpose of this paper is to: (1) find the relationship between surface temperature inside the green space and impact factors inside the green space; (2) find the relationship between GCI indicators and LST impact factors inside and outside the green space derived from the land cover; and (3) study the relationship between LST and the spatial patterns of green spaces. These two cities were selected for the purpose of cross-learning. With cross-learning, the results of this study will help the urban planners and managers to develop city layouts with green spaces of appropriate shape, size, and spatial distribution.

2. Materials and Methods

2.1. Study Area

The capital cities of China and Pakistan (Beijing and Islamabad, respectively) were selected for this study, as shown in Figure 1. Both cities were selected for cross-learning purposes. Beijing is a heavily urbanized city and is expanding rapidly as compared to Islamabad. Islamabad is a poorly studied area and is still at an early phase of growth. Although the present SUHI situation of Islamabad is better than Beijing due to low population and less built-up area, because it is a capital city of the country, it is expected to expand rapidly and may eventually face the same problems as Beijing.

Beijing is the capital of the People's Republic of China. It is located at 39°26′ N–41°30′ N latitude and 115°25′ E–117°30′ E longitude. The maximum elevation of the urban region is around 200 m, but the elevation of hilly areas varies from 200–2500 m. With a total area of about 16410 km^2, geographically Beijing has been divided into fourteen districts [43] (Figure 1). Beijing experiences four seasons yearly, and its climate is sub-humid warm temperate monsoon, with hot and humid summers and very cold and windy winter seasons. In addition, Beijing is one of the numerous large cities that are rapidly urbanizing and expanding. The phenomenon of urbanization is replacing natural land cover types (especially vegetation), and increasing the surface temperature of the core city area. The permanent population of Beijing reported in 1989 was approximately 11 million, but this figure exceeded 21 million in 2016. The rapid economic growth is also leading to a great pressure on the natural resources and environment of Beijing. The per capita Gross Domestic Product (GDP) of Beijing has increased from 4269 Yuan to 106,497 Yuan from 1989 to 2015 [43]. Beijing is currently facing many serious environmental problems, such as smog, air pollution, urban heat islands (UHIs), as well as

sand and dust storms. The proximate determinants of these problems are massive industrialization and rapid increase in urbanization, which are replacing green spaces—a very important factor in controlling UHI [44].
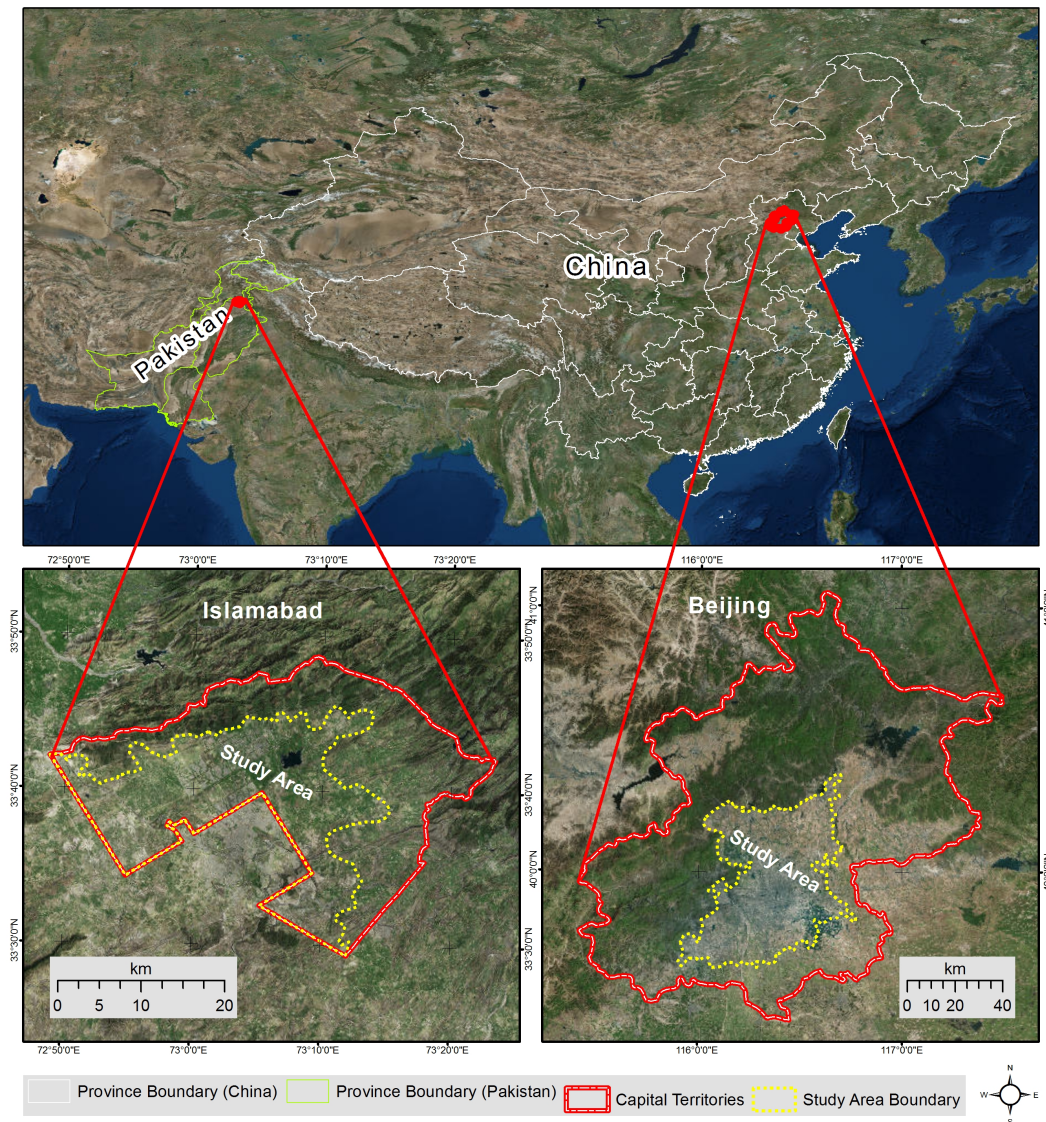
Figure 1. Location map of study area.

Islamabad is the capital city of the Islamic Republic of Pakistan. It is located between 33°28′12″–33°48′36″ N latitude and 72°48′36″ E – 73°24′ E longitude. The elevation of the urban areas of Islamabad varies between 400–600 m. The capital is flanked by the Margalla Hills in the northern side of the city (Figure 1). The area of Islamabad is about 906 km^2, and the total population is about 2 million [45]. Islamabad has a humid subtropical climate with four seasons: winter, summer, spring, and autumn. It is divided into four different zones: residential, commercial, diplomatic, and industrial. The overall environmental situation of the city is satisfactory, but some areas such as residential and industrial zones still need proper management to overcome the existing environmental problems and to avoid the potential future threats. The industrial zone is composed of different types of industries, such as pigments, oil units, paints, chemical or soap factories, marble factories, flour mills, steel mills, and pharmaceutical plants. The increasing emissions from industrial processes and automobiles are the primary sources of air pollution and rise in air temperature [46].

To study the urban green spaces, the most urbanized regions of Beijing and Islamabad were selected for this study.

2.2. Satellite Data Sources

The satellite imagery of Gaofen-1 (GF-1) and Landsat-8 Operational Land Imager (OLI) were used in the present study. The thermal infrared (TIR) bands of Landsat-8 were used to calculate LST, whereas land cover classification was done using GF-1 satellite imagery. To avoid phenological differences, shadows, and cloud cover, satellite data was acquired for the month of September 2015. The satellite images were pre-processed before LST calculation and land cover classification. Different pre-processing steps were applied, including atmospheric corrections, layer stacking, and area of interest (AoI) truncation. Specifications of satellite data used are given in Table 1.

Table 1. Satellite data specifications.

Satellite Name	Spectral Mode	Spatial Resolution (m)
Landsat-8 (OLI)	Multispectral	30×30
	Panchromatic	15×15
	Thermal Infrared	100×100
Gaofen-1 (GF-1)	Multispectral	8×8
	Panchromatic	2×2

2.3. Methodological Approach

The overview of satellite data and the methodological approach applied for this study are given in the flow diagram in Figure 2.
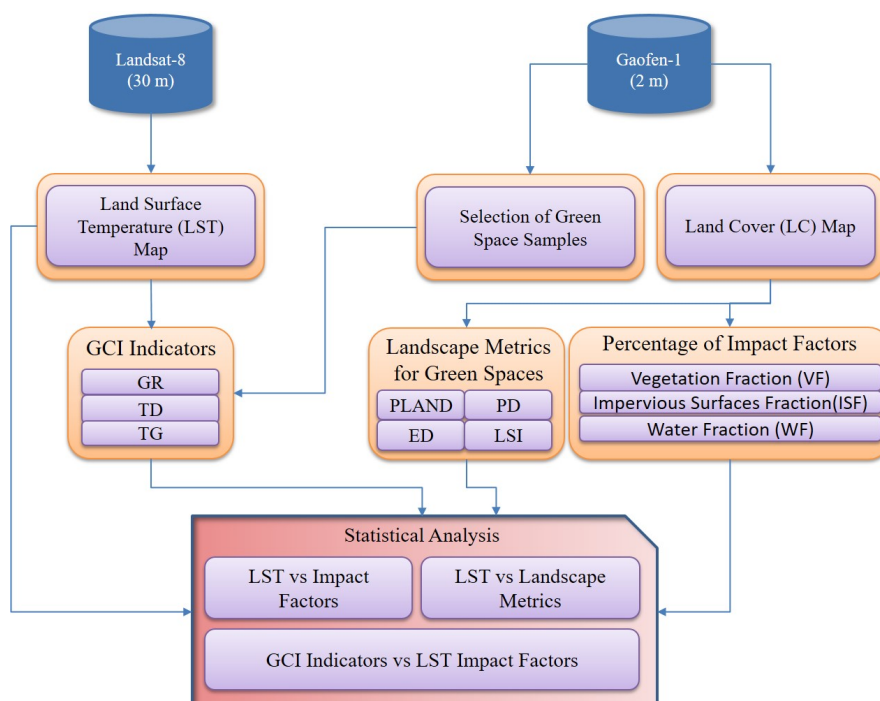
Figure 2. Methodological framework. ED: Edge Density; GCI: Green Space Cool Island; GR: Green Space Range; LSI: Landscape Shape Index; LST: Land Surface Temperature; PD: Patch Density; PLAND: Percentage of Landscape; TD: Temperature Difference; TG: Temperature Gradient.

2.4. Land Surface Temperature (LST) Retrieval

The three most commonly used methods for LST calculation from thermal bands are: (1) multi-channel or split-window algorithm; (2) multi-angle method; and (3) single channel method [47,48]. To calculate LST from the thermal infrared bands (TIRs) of Landsat-8, the split-window algorithm was applied [49,50]. The single-channel algorithms have been improved to estimate LST from the TIR bands of LST [51]. Wang et al. [52] upgraded the method of the mono-window algorithm of Qin et al. [53] to estimate LST from the TIR bands of Landsat-8. The mono-window algorithm only requires two atmospheric parameters; therefore, it is a simpler method compared to the split-window algorithm [52].

The split-window algorithm (SW) was applied to calculate LST for this study. Due to the significant reliability of the SW algorithm, it has a wider applicability. It uses the brightness temperatures of two TIR bands (band 10 and band 11 of Landsat-8) to calculate mean land surface emissivity, difference of land surface emissivity, and then to estimate LST [54]. This algorithm is explained below and split-window coefficients are given in Table 2:

$$LST = TB_{10} + C_1(TB_{10} - TB_{11}) + C_2(TB_{10} - TB_{11})^2 + C_o + (C_3 + C_4 W)(1 - \varepsilon) + (C_5 + C_6 W)\Delta\varepsilon, \quad (1)$$

where

C_0, C_1, C_2, C_3, C_4, C_5 and C_6 = the split-window coefficients;
TB_{10} = brightness temperature of band 10 (Kelvin K);
TB_{11} = brightness temperature of band 11 (Kelvin K);
ε = mean value of Land Surface Emissivity (LSE) of TIR bands;
W = content of water vapors in the atmosphere;
$\Delta\varepsilon$ = difference between LSE of bands 10 and 11.

Table 2. Split-window coefficients.

Constant	Value
C_0	−0.268
C_1	1.3780
C_2	0.1830
C_3	54.300
C_4	−2.238
C_5	−129.2
C_6	16.400

2.4.1. Brightness Temperature (T_B)

To calculate the brightness temperature (T_B), we need the Top of Atmosphere spectral radiance (ToA, L_λ). ToA was calculated by multiplying the corresponding thermal band with a multiplicative rescaling factor (0.000342) and adding the additive rescaling factor (0.1). It is represented by (A_L) and measured in Watts/(m^2*srad*μm)

$$L_\lambda = M_L Q_{cal} + A_L, \quad (2)$$

where

Q_{cal} = reflectance of band 10 or 11;
M_L = band-specific multiplicative rescaling factor;
A_L = the additive rescaling factor.

Thermal Digital Numbers (DNs) were converted to Brightness Temperature (T_B) by the process of calibration, and (T_B) was calculated for TIR bands 10 and 11 from the following algorithm:

$$T_B = \frac{K_2}{L_n \left[\left[\frac{K_1}{L_\lambda} \right] + 1 \right]},$$ (3)

where

K_1, K_2 = thermal conversion constants. These are different for both TIR bands and are given in the metadata files;

L_λ = radiance of Top of the Atmosphere (ToA).

2.4.2. Land Surface Emissivity (LSE)

LSE is an essential parameter to calculate LST, and was calculated by using the Normalized Difference Vegetation Index (NDVI) threshold method. The LSE calculation method is described below:

$$LSE = \varepsilon_s (1 - FVC) + \varepsilon_v FVC,$$ (4)

where

ε_v = vegetative emissivity value;

ε_s = value of the soil emissivity of corresponding bands; FVC = vegetation fraction [55].

The values of ε_v and ε_s are given in Table 3

Table 3. Vegetation and soil emissivity values for Landsat-8 (OLI) band 10 and band 11.

Emissivity	Band 10	Band 11
ε_s	0.971	0.977
ε_v	0.987	0.989

The vegetation fraction (FVC) for the study sites was calculated by applying the following equation:

$$FVC = \frac{NDVI - NDVI_s}{NDVI_v - NDVI_s},$$ (5)

where,

$NDVI$ = Normalized Difference Vegetation Index;

$NDVI_s$ = reclassified NDVI value for soil;

$NDVI_v$ = reclassified NDVI value for vegetation.

2.4.3. NDVI Threshold

Red and near-infrared (NIR) bands of Landsat-8 were used to calculate NDVI. The NDVI images were further reclassified into soil and vegetation to acquire the NDVIs and NDVIv, respectively. These classified images for study areas were used to compute FVC. The mean and difference of LSE for TIR bands were calculated from the following formulas:

$$\varepsilon = \frac{(\varepsilon_{10} - \varepsilon_{11})}{2},$$ (6)

$$\delta\varepsilon = \varepsilon_{10} - \varepsilon_{11},$$ (7)

where

ε = mean LSE;

$\delta\varepsilon$ = difference in LSE.

Finally, putting all of the above values into Equation (1) (SW algorithm), LST was calculated in Kelvin (K), and it was converted into °C by subtracting 273 from the calculated pixel values (see Figure 3).
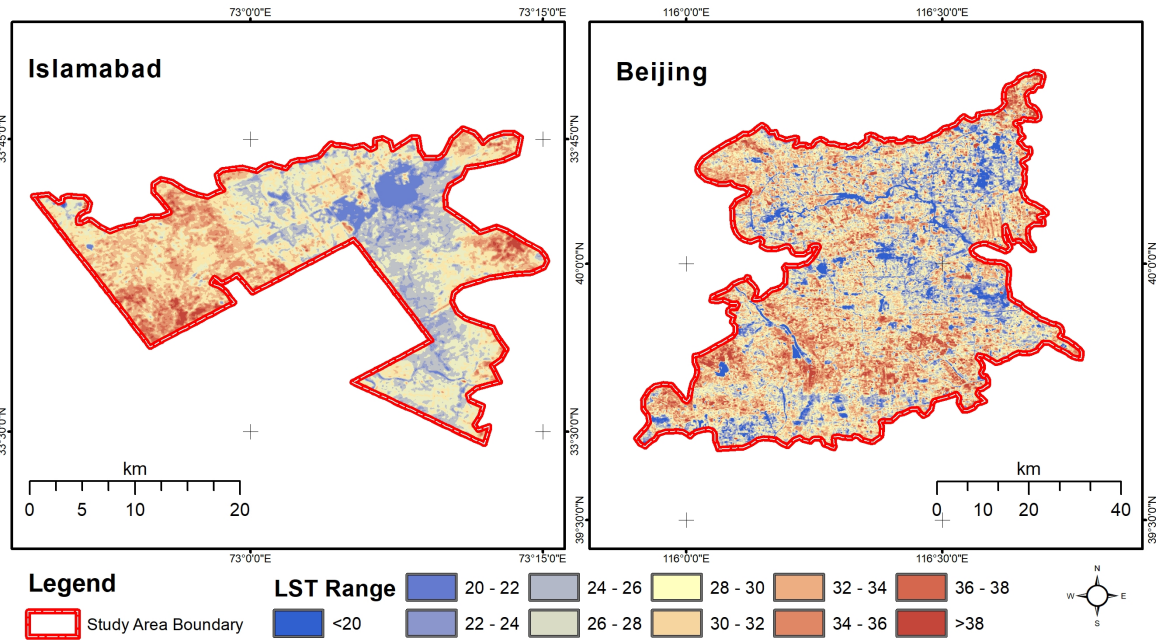

Figure 3. Land Surface Temperature of Islamabad and Beijing.

2.5. Statistical Approach

This section is composed of two parts: (1) scatter plots were drawn for visual interpretation of the data to analyze whether or not there is any relationship between LST and green spaces. Pearson's coefficient (r) was calculated to determine the degree of relationship or association. Pearson's coefficient (r) is the square root of the coefficient of determination (R^2); (2) normalized mutual information (NMI) among LST and landscape metrics was calculated to determine the amount of information shared between the two parameters. In probability or information theory, mutual information (MI) is defined as the mutual dependency or amount of information shared between two random variables [56,57]. Its concept is closely related to the entropy of a random variable. The Shannon entropy $H(X)$ of a continuous random variable X is expressed as below:

$$H(X) = - \int_s p(x) \, log(px) dx,$$

where

$x \in s$ and $p(x)$ = probability distribution for whole function;
s = support of variable.

The formal definition of mutual information for two continuous random variables is given below:

$$I(x,y) = \int_x \int_y p(x,y) log \left(\frac{p(x,y)}{p(x)P(y)} \right) dx \, dy, \tag{8}$$

where

$p(x)$ and $p(y)$ = marginal probability density functions;
$p(x,y)$ = joint probability density function of x and y.

The Shannon entropy $H(X)$ for a discrete random variable X is defined as

$$H(X) = - \sum_{x \in \Omega} p(x) \, log(px),$$ (9)

where

$p(x)$ = probability of an event for $x \in \Omega$ of possible values from a definite set Ω.

The frequency distribution of discrete events can be constructed from probability distributions in the form of a histogram [55,58]. To define the mutual information for discrete random variables, the defined integral will be replaced with a summation

$$I(x,y) = \sum_{y \in Y} \sum_{x \in X} p(x,y) log \left(\frac{p(x,y)}{p(x)P(y)} \right),$$ (10)

where

$p(x)$ and $p(y)$ = marginal probability density functions;
$p(x,y)$ = joint probability density function of x and y.

Separately, $p(x)$ and $p(y)$ can be defined as

$$p(x,y) = P(X = x, Y = y),$$ (11)

and it can be defined as

$$p(x) = \sum_{y \in A} p(X = x, y),$$ (12)

$$p(y) = \sum_{x \in A} p(x, Y = y).$$ (13)

X and Y are the marginal probability distributions functions. $I(x,y)$ cannot be a negative quantity because it is the measurement of the total amount of information shared between the two variables. $I(x,y)$ can be zero if the variables are statistically independent; higher values of $I(x,y)$ increase the dependence between the two variables [59,60]. Normalized mutual information [57] is defined below:

$$C_{XY} = \frac{I(X;Y)}{H(Y)} \quad and \quad C_{YX} = \frac{I(X;Y)}{H(X)}.$$ (14)

The above equations can derive linear and nonlinear relationships between variables. Normally, it is expressed as the "asymmetric dependency coefficient (ADC)" [57,61]. Due to asymmetric property, the above equations will produce unequal values, so symmetric normalized mutual information is proposed [62,63]:

$$NI(X,Y) = 2\frac{I(X;Y)}{H(Y) + H(X)} \quad and \quad NI(X,Y) = \frac{I(X;Y)}{\sqrt{H(X)H(Y)}}.$$ (15)

It is important to mention here that the MI of two random variables is always less than their entropies $(I(X;Y) < H(Y)$ and $I(X;Y) < H(X))$ because the shared information of both variables can never be greater than the individual information, $0 <= C_{XY} <= 1$. $C_{XY} = 0$ shows no correlation between X and Y, and $C_{XY} = 1$ means that X and Y are perfectly correlated. Equation (14) is applied to compute the normalized mutual information between landscape metrics and LST because the purpose of this study was to determine the mutual correlation between urban thermal properties and vegetation patterns. Land Surface Temperature was used as a reference variable.

2.6. Land Cover Classification

GF-1 satellite imagery was used for the land cover classification. An object-based image analysis approach was applied to extract the land cover classes. Satellite data was classified into four major classes (vegetation, built-up area, water, and others) for statistical analysis. Land cover map of Beijing and Islamabad is shown in Figure 4 and Table 4 indicate land cover statistics.

Table 4. Land cover statistics.

Class Name	Islamabad (%)	Beijing (%)
Vegetation	48.59	21.83
Built-up area	19.58	64.26
Water	1.58	1.12
Others	30.25	12.79
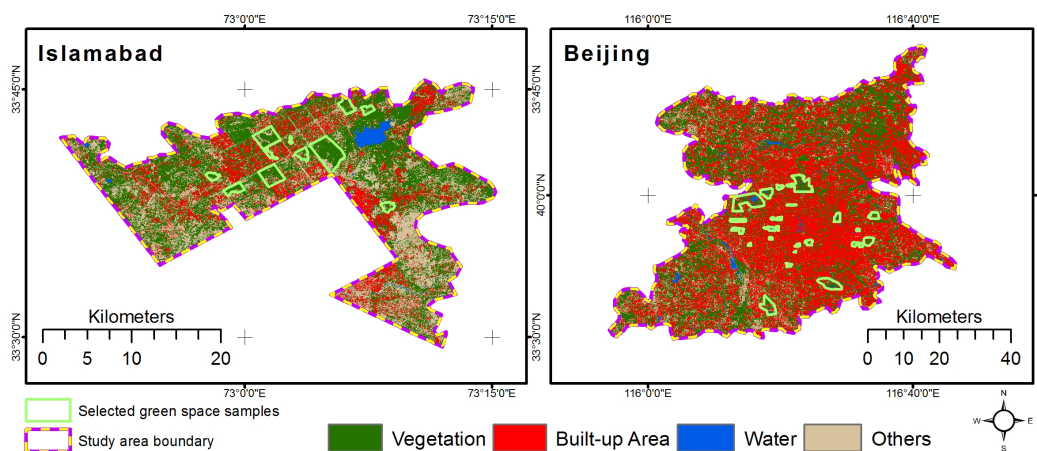
Figure 4. Land cover map of the study area.

The accuracy was assessed by selecting randomly sampled points of some homogeneous areas of all four classes. These points were taken from the centers of the classified segments. The selected points were verified using high-resolution data of Google Earth and used as a reference data [64,65]. The land cover accuracies of Beijing and Islamabad are given in Tables 5 and 6.

Table 5. Accuracy assessment of the classified map of Islamabad.

Class Name	No. of Samples	Total Sample Area (Ha)	User's Accuracy (%)	Producer's Accuracy (%)
Green space	85	78.2	89.43	88.24
Built-up area	42	31.5	85.81	82.65
Water	12	9.1	80.34	85.41
Others	28	20.9	79.01	77.34
Total	167	139.7		
Overall accuracy	83.6			

Table 6. Accuracy assessment of the classified map of Beijing.

Class Name	No. of Samples	Total Sample Area (Ha)	User's Accuracy (%)	Producer's Accuracy (%)
Green space	147	139.6	90.13	91.39
Built-up area	110.1	31.5	84.81	85.51
Water	10	7.3	85.37	79.34
Others	61	44.7	75.72	81.46
Total	341	301.7		
Overall accuracy	84.01			

*2.7. Green Space Characteristics, Indicators, and Impact Factors*

2.7.1. Green Space Spatial Patterns

Four metrics were calculated to measure and describe the composition and configuration of urban green spaces [37,66]. The four commonly occurring metrics were selected to correlate urban green space patterns with LST [67]. The selected metrics include: PLAND, ED, PD, and LSI [66]. The selected metrics are given in Table 7. PLAND is a compositional element that describes the variety and abundance of green spaces, whereas ED, PD, and LSI are the configurational elements used to describe the spatial distribution of green spaces. These metrics were selected on the principle that they are easy to calculate, easy to interpret, theoretically and practically important, and have minimal redundancy [66]. These metrics provide the complementary information about vegetation configuration and composition.

The spatial patterns of selected metrics were calculated using FRAGSTATS. FRAGSTATS is an open source program (http://www.umass.edu/landeco/research/fragstats/fragstats.html) used for the structural analysis of landscapes. A moving window sampling strategy was applied to generate new grids of selected metrics. In moving window analysis, a window of specified size and shape passes over the landscape having positively valued cells, calculates a new grid for each metric, and returns the focal cell. This process continues until every positively-valued cell inside the window is assessed. A square window with a side length of 1-km^2 was moved over the green spaces class of land cover with 8-cell rule [66]. The calculated metrics are shown in Figure 5. The green space spatial patterns were then resampled based on a 1×1 km^2 grid.

Table 7. Description of landscape metrics calculated for vegetation configuration and composition.

Landscape Metric	Calculation	Description
Percentage of Landscape *(Compositional)*	PLAND = $100/A \times \sum_{i=1}^{n} a_i$	Percentage of landscape quantifies the proportional abundance of green spaces in the landscape (%)
Edge Density *(Configurational)*	ED = $(\frac{10,000}{A}) \sum_{i=1}^{n} e_i$	Total length (border not included) of all edge segments of green space per hectare (m/ha)
Patch Density *(Configurational)*	PD = $n/A \times 10^6$	Number of green space patches divided by total landscape area (n/km^2)
Landscape Shape Index *(Configurational)*	LSI = $0.25 \sum_{k=1}^{m} (\frac{e_{ik}}{A})$	It gives a standardized measure of edge density or total edge, which adjusts the size of a landscape
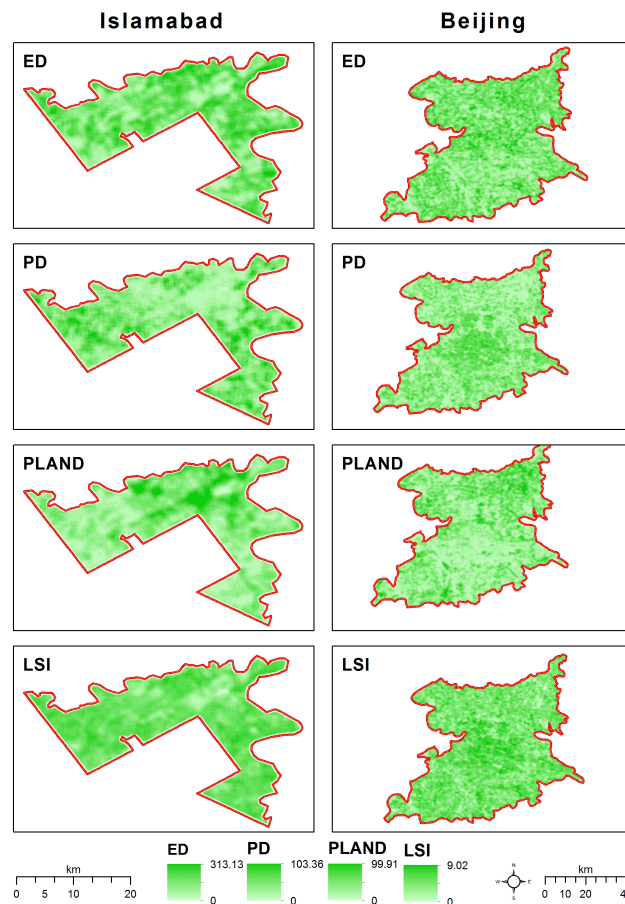
Figure 5. Landscape metrics calculated from green spaces of Beijing and Islamabad.

2.7.2. GCI Indicators and LST Impact Factors

The cooling effect is estimated by calculating the difference of LST between each GCI and its surrounding area. In this study, the surrounding areas of all the green spaces were buffered with an equal distance of 30 m from a green space boundary up to 1500 m. The mean surface temperature was calculated within each buffer zone to form a temperature curve of each green space sample.

According to the Du et al. (2017) study [68], the GCI indicators are:

1. Green Space Range (GR): The distance between green space edge and the first drop in temperature outside the green space. It is measured in km.
2. Temperature Difference (TD): The LST difference between the first drop in temperature and the average temperature of the green space interior. It is measured in °C.
3. Temperature Gradient (TG): The temperature drop per unit distance in the surrounding areas. It is measured in °C/km^2.

The following LST impact factors are selected to explore the impact of GCI on its surrounding area:

1. Green Space Area (GSA)
2. Vegetation fraction within the green space boundary (VFi)
3. Water body fraction within the green space boundary (WFi)
4. Impervious surface fraction within the green space boundary (ISFi)
5. The combined effect of vegetation and water fractions within the green space boundary (VWFi)
6. Vegetation fraction outside the green space boundary (VFo)
7. Water body fraction outside the green space boundary (WFo)
8. Impervious surface fraction outside the green space boundary (ISFo)
9. The combined effect of vegetation and water fractions outside the green space boundary (VWFo)

3. Results

3.1. Correlation between Green Space Spatial Patterns and LST

The LST and green space spatial patterns data was resampled based on a 1-km^2 grid. The main purpose of the study is to determine the degree of relationship or association between LST and green space characteristics; therefore, scatter plots were drawn only to investigate whether any relationship (trend) between LST landscape metrics exists or not, and Pearson's coefficient (r) was calculated to measure the degree of relationship or association between green space spatial patterns and LST. It can be seen from the scatter plots (Figure 6) that some metrics look flat (no specific trend) and some of them do have a slight trend, but $R^2 < 0.36$ in all cases. Therefore, the relationships between LST and green space spatial patterns do not seem to be statistically significant. The R^2 values of (Figure 6) suggest that PLAND has a weak negative linear relationship with LST for both cities. Among other metrics, PD and LSI of Islamabad and ED of Beijing show very weak linear positive relationships with LST. PD and LSI of Beijing and ED of Islamabad do not show any trend (negligible, $R^2 < 0.1$).

Figure 6. Correlation between LST and landscape metrics for Islamabad and Beijing.

Although the relationship between LST and the spatial patterns of urban green spaces is not sufficiently statistically significant to draw meaningful and logical conclusions, a weak relationship exists between some landscape metrics and LST, which can be further explored using other statistical measures to get some useful information. Pearson's coefficient was then calculated to measure the degree of relationship or association present between LST and green space spatial patterns. Relatively better relationships between LST and green space spatial patterns were displayed by Pearson correlation (see Table 8).

Table 8 illustrates that PLAND has a moderate negative correlation for both cities. PD shows a weak positive correlation for Beijing and moderate positive correlation for Islamabad. ED of Beijing indicates a week negative correlation, whereas LSI of Islamabad has a weak positive correlation with LST. ED of Islamabad and LSI of Beijing show a very weak correlation ($r < 0.1$). Pearson's correlation coefficient suggests that both the configuration and composition of urban green spaces play a significant role in the mitigation of surface heat, to a certain extent. Green space composition has a slightly stronger impact on LST than green space configuration, as LST and green space composition have stronger correlation as compared to green space configuration. Pearson's correlation depicts a better relationship than two-dimensional scatter plots. However, both are conventional methods.

Table 8. Pearson's correlation between landscape metrics and LST for Islamabad and Beijing.

Landscape Metrics	Islamabad	Beijing
PLAND	−0.59	−0.60
ED	−0.20	−0.37
PD	0.43	0.26
LSI	0.39	0.08

Correlation is significant at the 0.01 level.

NMI, an unconventional method, was then utilized to explore the relation between LST and green space spatial patterns. NMI is not commonly applied to urban ecosystem investigation, but it can be very useful if conventional methods do not show conclusive results. NMI and Pearson's correlation both measure the degree of association or relationship between the two variables. However, Pearson's correlation only measures the linear association, while NMI quantifies the total association (both linear and nonlinear) between the two variables. According to information theory, NMI is a measure of the "mutual dependence" or "amount of information" between two random variables. In remote sensing, NMI is extensively used for image registration (see Table 9).

Table 9. Normalized mutual information (NMI) between LST and landscape metrics.

| Landscape Metrics	Land Surface Temperature (LST)	NMI of Islamabad	NMI of Beijing
PLAND		0.77	0.76
ED	LST	0.75	0.71
PD		0.57	0.38
LSI		0.66	0.51

As NMI determines the amount of information shared between the two variables, it is therefore a non-negative quantity. Overall results of NMI show that a significant amount of information is shared between landscape metrics and LST. The NMI of landscape metrics and LST also determined that vegetation composition is slightly more important than its configuration. Mutual correlation of PLAND, ED, PD, and LSI with LST demonstrated that all these elements share a large amount of information, with varying degrees of impact. PD and LSI seem to have a less deterministic effect on LST as compared to PLAND and ED.

3.2. Characteristics of Green Spaces and GCI Effect

For this study, 22 green space samples were selected from Beijing, while 11 samples were selected from Islamabad. The average inside surface temperature of all green space samples, for Beijing was calculated to be 29.03 °C, and for Islamabad was 29.52 °C. Outside the green space samples, average surface temperature was 31.48 °C and 30.91 °C for Beijing and Islamabad, respectively, obviously higher than the inside temperature.

The examples of LST curves are presented in Figure 7. These curves show that the temperature around the green spaces rises with increasing distance from the green space. The temperature rise slows down with further increase in distance, and ultimately starts decreasing. The distance between the green space edge and the last point before the first drop in temperature defines GR, while the difference in temperature from the green space edge to the last point before the first drop in temperature defines TD, which is indicated by a red line in Figure 7.

The results of this study prove that green spaces provide cool island effects. GSA varied from 0.1–20.5 km^2 and 0.15–6.93 km^2 for Beijing and Islamabad, respectively, whereas the average green space LST varied from 26.8–31.65 °C and 27.36–32 °C for Beijing and Islamabad, respectively. Average area per patch for Beijing and Islamabad was 3.9 km^2 and 1.9 km^2, respectively. TD for Beijing varied between 0.85–4.92 °C, with an average value of 2.98 °C. For Islamabad, the TD range was 0.17–4.04 °C with an average value of 1.53 °C for Islamabad. TG varied between 0.1–22.4 °C/km with an average value of 3.6 °C/km for Beijing, and 0.17 °C/km – 7.56 °C/km with an average value of 1.72 °C/km for Islamabad.
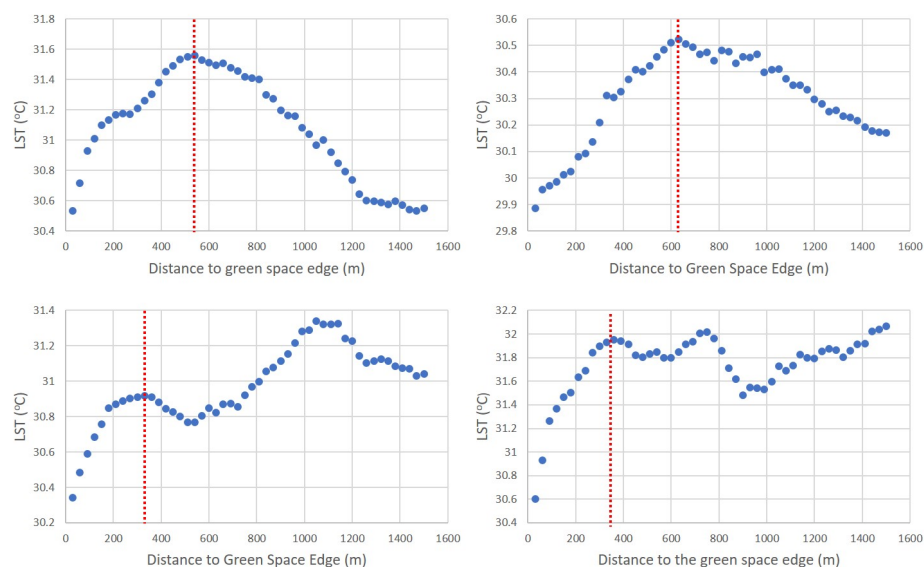

Figure 7. Examples of temperature curves drawn from the 30 m buffers outside the polygons.

3.2.1. Relation between Surface Temperature of Green Space and Impact Factors

Figures 8 and 9 show the scatter diagrams and Pearson's correlation (r) calculated for LSTs and impact factors inside the green space samples. The Pearson's coefficient (r) values indicate that the combination of water and vegetation (VWFi) is the most important impact factor, as it has a significant negative correlation with LSTs. ISFi shows a moderate linear positive relationship with green space temperature for Beijing and a strong positive correlation with Islamabad. Therefore, higher ISFi leads to higher surface temperature of green space (Figures 8 and 9) for both Beijing and Islamabad. VFi of green spaces is negatively correlated with LST. This relationship is moderate for Islamabad, but weak in the case of Beijing. GSA shows almost no relationship when GSA is less than 5 km^2. After 5 km^2,

it shows a somewhat linear correlation with LST. Similarly, for Islamabad, after 2 km^2 it shows a linear relationship. Twelve of the green space samples of Beijing contain water bodies, whereas no green space sample in Islamabad contains a water body. Therefore, 12 samples of Beijing were extracted for further analysis to find the connection between WFi and LST of green space. WFi also shows a a moderate negative relationship with LST.

The combination of vegetation and water (VWFi) plays the most important role in the mitigation of LST effects among these impact factors, as it shows a strong correlation with green space temperature. The results indicate that, as the amount of vegetation and water inside the green space increases, the LST significantly decreases. The combined effect of vegetation and water body is observed to be the strongest impact factor in minimizing the surface heat.
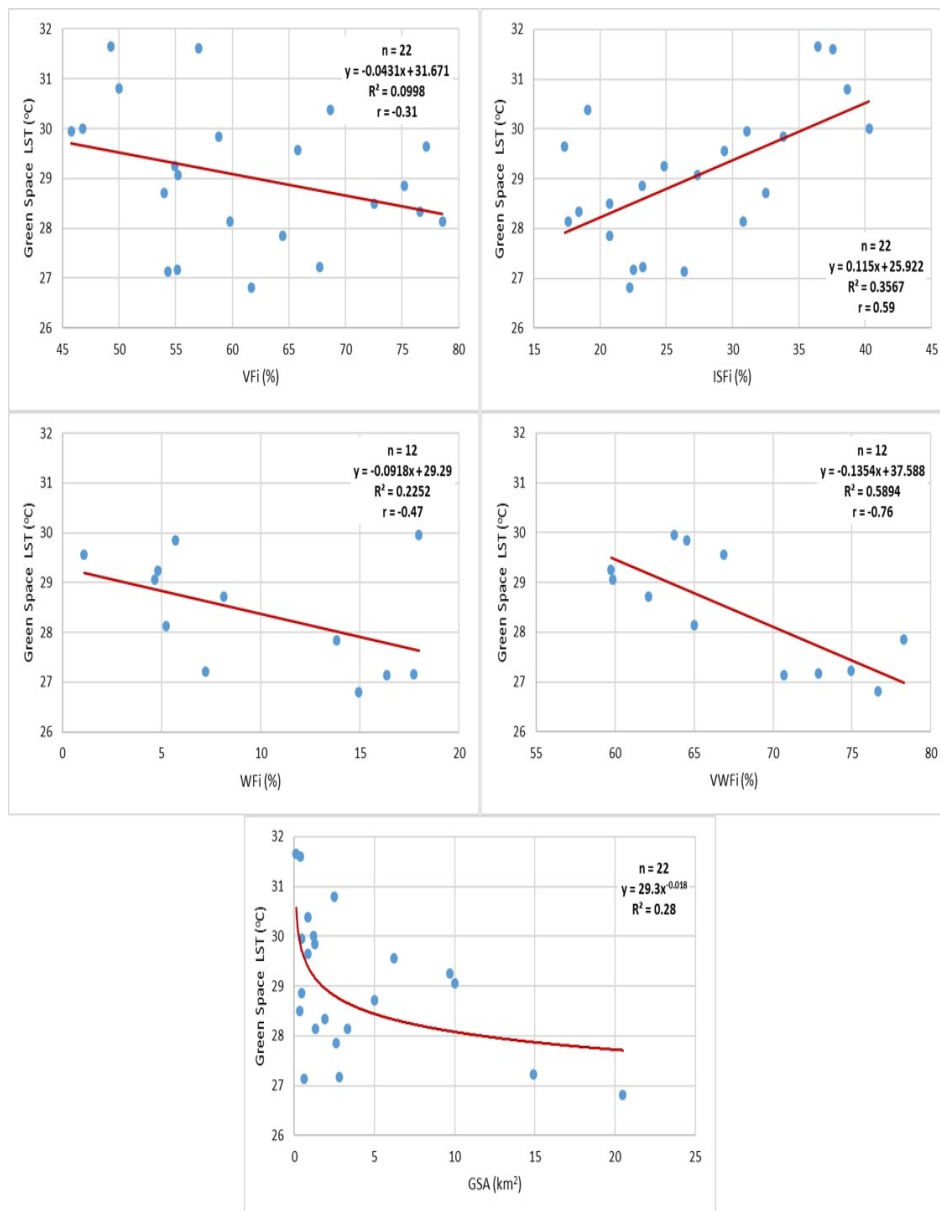
Figure 8. Correlation between LST and impact factors of Beijing. GSA: Green Space Area.
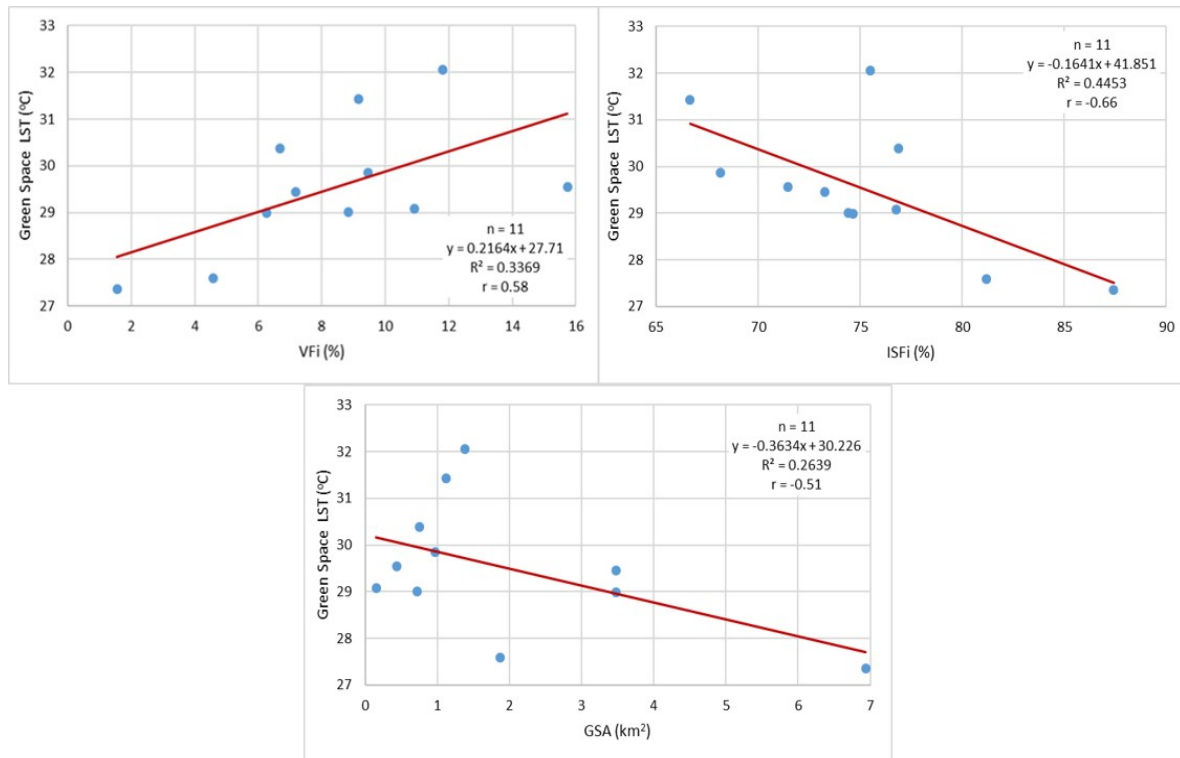
Figure 9. Correlation between LST and impact factors of Islamabad.

3.2.2. Relation between LST Impact Factors and GCI Indicators

Tables 10 and 11 show the Pearson correlation between GCI and impact factors. GR is positively correlated with GSA, WFi, VWFi, VFo, WFo, and VWFo, while it is negatively correlated with ISFi and ISFo for both Beijing and Islamabad. VFi and GR do not have any significant correlation for Beijing, but have a strong positive correlation for Islamabad. Similarly, TD is positively correlated with all of the impact factors except ISFi, which is negatively correlated for both Beijing and Islamabad. The correlation between VFo and TD is very weak. TG is positively correlated with ISFi, WFi, ISFo, WFo, and negatively correlated with all other impact factors for both Beijing and Islamabad. VFi is negatively correlated with TG for Beijing, and positively correlated for Islamabad.

Table 10. Pearson's correlation between impact factors and GCI indicators of Beijing. ISFi: impervious surface fraction within the green space boundary; ISFo: impervious surface fraction outside the green space boundary; VFi: vegetation fraction within the green space boundary; VFo: vegetation fraction outside the green space boundary; VWFi: combined effect of vegetation and water fractions within the green space boundary; VWFo: combined effect of vegetation and water fractions outside the green space boundary; WFi: water body fraction within the green space boundary; WFo: water body fraction outside the green space boundary.

GCI	GSA	VFi	ISFi	WFi	VWFi	VFo	ISFo	WFo	VWFo
GR	0.72	0.042	−0.32	0.37	0.66	0.57	−0.32	0.73	0.77
TD	0.18	0.14	−0.36	0.65	0.64	0.1	0.18	0.62	0.6
TG	−0.43	−0.21	0.22	0.57	−0.06	−0.51	0.34	0.23	−0.3

Correlation is significant at the 0.05 level.

Table 11. Pearson's correlation between impact factors and GCI indicators of Islamabad.

GCI	GSA	VFi	ISFi	VFo	ISFo
GR	0.87	0.67	−0.68	0.28	−0.3
TD	0.48	0.81	−0.69	0.09	0.06
TG	−0.45	0.16	0.28	−0.06	0.25

Correlation is significant at the 0.05 level.

4. Discussion

This study applied different statistical methods to explore the influence of urban green spaces on the thermal environment of Beijing and Islamabad. Four landscape metrics were used to investigate the relationship between spatial patterns of urban green spaces and LST. This relationship demonstrated that both vegetation composition and configuration play an important role in the mitigation of SUHI effects to a certain extent, but vegetation composition influences SUHI distribution more effectively. The areas surrounding green space affect GCI in different ways. The effect of urban green spaces on SUHI intensity varies across climatically different regions (i.e., Beijing and Islamabad). The results of this study were found to be consistent with some previous studies on urban green spaces and surface temperature [38,68–70].

4.1. Green Space Spatial Patterns and LST

The results of Section 3.1 indicate that both green space composition and configuration affect the SUHI phenomenon to a certain degree, though the effect of green space composition is slightly greater than the effect of its configuration. These results are consistent with a number of studies [31,38,40,69]. The NMI results also show that PLAND is the most effective parameter, as it shares maximum information with LST amongst the selected metric and is also supported by the study of Maimaitiyiming et al. (2014) [39].

PLAND is a composition element of urban green spaces and Pearson's coefficient (r) indicates a negative correlation with LST, which is comparatively stronger than the other three selected metrics. Therefore, a greater percentage of vegetation can help mitigate SUHI phenomena more effectively. These results are also consistent with a number of previous studies [12,71,72]. Edge density is an important parameter of green space configuration. ED and LST have a weak negative correlation for Beijing and a very weak one for Islamabad. Although ED has a weak correlation with LST, it might still affect SUHI intensity to a certain degree. The negative correlation between ED and LST indicates that plantation with equal distribution and in a specific order can reduce the surface thermal impacts. These results are similar to some previous studies [24,72]. The positive correlations of patch density with LST demonstrate that more fragmentation leads to higher temperature [12,35,38,69,73]. Cao et al. [31] demonstrated that when the patch density increases, the mean patch size will decrease, and ultimately increases the total patch edges. Thus, the increase in patch density can affect surface temperature by both an increase in patch edges or decrease in mean patch size. In addition, one larger continuous vegetation patch produces a stronger cooling effect than several small patches, even if the total area of small patches is equal to the area of the larger continuous vegetation patch. Therefore, surface temperature may increase due to the decrease in mean patch size. Meanwhile, if total patch edges increase, it can increase the energy flow as well as exchange between a vegetation patch and its surroundings to provide more shade for surrounding areas, and ultimately decreases the surface temperature [31,40]. Landscape Shape Index also indicates a positive correlation with LST, particularly for Islamabad. Therefore, irregularly shaped urban green spaces increase the surface temperature, which is consistent with the conclusions of Zhibin et al. [38].

Urban green spaces decrease the surface temperature by the process of evapotranspiration because vegetation has a lower thermal inertia compared to bare soil and impervious surfaces [24,72]. It also provides shade that protects the land surfaces from solar radiation [71]. A different magnitude of the

same trend of the relationship between green space spatial patterns and LST was observed in both Beijing and Islamabad, which indicates that the local climatic conditions, tree species, urbanization, population density, and vegetation cover affect the strength of the cooling effect. There is no countable study on SUHI for Islamabad; therefore, the results for Islamabad cannot be compared with local studies. Regardless, the current study can help other researchers for further studies in the future. Results of normalized mutual information also indicate that a considerable amount of information (NMI > 0.5 for all metrics except PD of Beijing) is shared between green space spatial patterns and LST. It is evident LST and green space patterns have mutual dependency, and can affect the SUHI phenomenon to a certain degree.

4.2. GCI Indicators and LST Impact Factors

In this study, the green space samples are mostly covered with three land cover classes: impervious surfaces, vegetation, and water bodies. According to the results of Section 3.2.1, high WFi, low ISFi, and large GSA will help to reduce the green space's temperature. These results coincide with the research conclusions of Chang et al. and Cao et al. [31,72]. VFi show a weak correlation with surface temperature of the green space samples of Beijing, which coincides with the results of Du et al. [68] and is different from the results of Kong et al. [74]. However, the correlation between VFi and LST of Islamabad is better than Beijing, which coincides with the research conclusions of Kong et al. [74]. The theory behind these results is quite logical; larger GSA covers a greater amount of vegetation, so transpiration and photosynthesis use more energy and lower the LST [32]. The higher LST of impervious surfaces is due to the higher thermal conductivity of the material used [75]. The higher thermal capacity of the water body leads to lower surface temperature [42]. Vegetation and water both have higher thermal capacities compared to bare soil and impervious surfaces. The percentage of vegetation had a limited number of samples for Islamabad and had high variation. Therefore, the correlation of LST with vegetation varied in strength for Beijing and Islamabad. However, if we count the total percentage of water body and vegetation within the green space samples of Beijing as a single variable, it shows a very strong negative correlation with LST. The results indicate that the LST of green spaces can be mitigated by reducing the impervious surfaces or by increasing the percentage of water body and vegetation.

In Section 3.2.2, the Pearson correlation between impact factors and GCI indicators indicate that the GR will be longer if green space covers a large area, high vegetation and water fraction inside or outside the green space, because the combined effect of vegetation and water (VWF) shows a strong correlation with GR. This trend coincides with the conclusions of Kong et al. and Chang et al. [42,74]. As green space samples of Islamabad do not have water bodies inside of them, we analyzed only for impervious surfaces and vegetation fraction. High ISFi and ISFo will lead to short GR (see Table 10). TA is positively correlated with all of the impact factors except ISFi. The trend of this correlation is the same for both Beijing and Islamabad. The results of this correlation coincide with the conclusions of Du et al. [68]. The research conclusions of Du et al. [68] indicate a negative correlation between impervious surfaces and TA regardless of whether it is inside or around the green spaces, but the present study shows a very weak positive correlation between ISFo and TA, which is different from the conclusions of Du et al. [68]. TG is mainly affected by GSA, percentage cover of water and vegetation inside and outside the green space both in Beijing and Islamabad. Most of these results are almost identical to the conclusions of Du et al. [68] except VFi, which shows negative correlation with TG. The combined effect of vegetation and water (VWFo) outside of the green spaces indicates a negative correlation, while VWFi does not show any trend with TG. The high WFi and WFo lead to a large value of TG for a green space. If the intensity of radiation remains the same, the green space—due to its high transpiration, photosynthesis, thermal capacity, specific heat capacity, and low effusivity—will have a lesser increase in LST as compared to its surroundings. Thus, the difference in temperature between inside and outside of a green space is generated and the hot air of the urban areas flow towards green spaces. The air surrounding the green spaces does not flow outside, and generates high pressure areas,

which maintain the cooler micro climate of green spaces. The water bodies increase the GCI efficiency more effectively. This is because water bodies have a strong cooling effect and serve as an extra source of cooling. The water bodies in the green space samples of Islamabad are missing; therefore, in the future, the urban planners of Islamabad should keep in mind that the combined effect of water and vegetation adds an extra cooling effect and increases GCI efficiency.

The cooling effect of vegetation and water could be explained based on different thermal properties. Vegetation has a lower thermal effusivity as compared to water and impervious surfaces, which signifies a slower process of heat emission from vegetation to the surrounding environment, and thus keeps the surrounding areas cooler for a longer period as compared to other land surface features. Similarly, higher thermal capacity and specific heat capacity of vegetation as compared to impervious surface indicate that a higher heat energy is needed to raise the temperature of UGSs. Briefly, higher thermal capacity, higher specific heat capacity, and lower thermal effusivity make UGSs a potential heat sink to keep the surrounding area cooler, and the higher thermal conductivity and higher specific heat capacity of water as compared to impervious surfaces makes it an effective heat sink [76].

4.3. Urban Planning Implications

Previous studies have already established that urban green spaces play an important role in SUHI mitigation [31]. Urban green spaces provide green space cool islands that help to minimize the LST of green spaces as well as their surrounding areas. The Chinese government has taken several initiatives for Beijing. "Urban Green space Work Plan (UGWP)" [77], "Beijing's 13th Landscape and Greening Plan (LGP)" [78] and the "Wedge green belt" project [79] are worth mentioning, which are some prominent steps taken by the Chinese Government for Beijing. It is planned to increase the canopy of tree cover to minimize the urban thermal impacts in the city [31,79]. Islamabad needs to follow in the footsteps of Beijing for the mitigation of SUHI effects. Unlike Beijing, Islamabad is not a mega city. Nevertheless, its rapid expansion may lead towards a similar problem in the near future.

To reduce the SUHI effects in the landscape by urban green spaces, urban designers should consider following important points: (1) regularly-shaped green spaces, plantation with equal distribution and less fragmentation; (2) increase in the GSA by considering the threshold—the SUHI mitigation efficiency increases after a certain GSA threshold value is reached; and (3) increase in water bodies percentage inside and around the green spaces to strengthen the cooling effect and efficiency with the help of GCI; just like Beijing, some artificial lakes need to be constructed within urban green spaces when designing the urban layout of Islamabad in the future.

5. Conclusions

With the rising trend of urbanization, increasing the vegetation cover in urban centers is very difficult. Consequently, vegetation arrangements can play an important role. Islamabad is a small city when compared to Beijing, yet its population is increasing rapidly, thus allowing the urban periphery to expand with time. Our results present some interesting findings.

(1) Complex shapes of green space and more fragmentation supports the SUHI phenomena because green spaces with square shape, less fragmentation, and a greater percentage of vegetation contribute to reducing the surface thermal impacts.
(2) Increase in the GSA by considering the threshold (2-km^2 for Islamabad and 5-km^2 for Beijing) increases the green space efficiency because, when GSA crosses a certain threshold, the SUHI mitigation efficiency starts increasing.
(3) The green space efficiency depends on interior characteristics as well as those of the surrounding environment. To strengthen the cooling effect and efficiency with the help of GCI, urban designers should consider the increase in vegetation fraction, decrease in impervious surfaces fraction, and increase the water bodies fraction inside and around green spaces.
(4) When designing the future urban layout of Islamabad, the construction of artificial lakes within urban green spaces would be beneficial, as is the case with Beijing.

Islamabad is a poorly studied area in the field of urban green spaces and surface heat islands. Hence, the current study will be helpful to understand how LST impact factors influence GCI indicators inside and around its green spaces. The conclusions will be helpful for urban landscape designers in the design of future city layouts. The limitations of this study include: less green space samples in Islamabad (Islamabad has few green spaces inside the urban area). Lack of reference data might have affected the accuracy of results. Both cities are very different in urban area size, population, climate, socioeconomic activities, and vegetation types; therefore, it is very difficult to compare them. However, the results might be helpful in cross-learning.

Author Contributions: Shahid Naeem was the leader of this work. He proposed the idea, processed data, compiled results and wrote this manuscript. Cao ChunXiang supervised with some fruitful ideas to make this work meaningful. Waqas A. Qazi and Mehdi Zamani developed the NMI program using MATLAB (Version R2016b, MathWorks, Natick, MA, USA). Bipin Kumar Acharya and Wei Chen supported in compiling results and writing and revising the manuscript. Asid Ur Rehman provided his technical inputs on conducting statistical analysis and assisted in their interpretation.

Conflicts of Interest: The authors declare no conflict of interest.

References

1. Frank, A. Tracing socioeconomic pattern of urban development: issues, problems and methods of spatio-temporal urban analysis. In Proceedings of the Geoinformatics Conference, Ann Arbor, MI, USA, 10–12 March 1999; pp. 1–12.

2. Orville, R.E.; Huffines, G.; Nielsen-Gammon, J.; Zhang, R.; Ely, B.; Steiger, S.; Read, W. Enhancement of cloud-to-ground lightning over Houston, Texas. *Geophys. Res. Lett.* **2001**, *28*, 2597–2600.

3. Meyer, W.B.; Turner, B.L. *Changes in Land Use and Land Cover: A Global Perspective*; Cambridge University Press: Cambridge, UK, 1994; Volume 4.

4. Grove, J.M.; Burch, W.R. A social ecology approach and applications of urban ecosystem and landscape analyses: A case study of Baltimore, Maryland. *Urban Ecosystems* **1997**, *1*, 259–275.

5. Breuste, J.; Feldmann, H.; Uhlmann, Q. *Urban Ecology*; Springer: Berlin, Germany, 1998.

6. Bhatta, B. *Analysis of Urban Growth and Sprawl from Remote Sensing Data*; Advances in Geographic Information Science; Springer-Verlag: Berlin/Heidelberg, Germany, 2010.

7. Moriyama, M.; Tanaka, T.; Iwasaki, M. The mitigation of UHI intensity by the improvement of land use plan in the urban central area: Application to Osaka City, Japan. In Proceedings of the Second International Conference on Countermeasures to Urban Heat Islands (SICCUHI), Berkeley, CA, USA, 21–23 September 2009.

8. Freire, M. Urban planning: Challenges in developing countries. In Proceedings of the International Congress on Human Development, Madrid, Spain, 3–5 August 2006.

9. Stewart, I.D. A systematic review and scientific critique of methodology in modern urban heat island literature. *Int. J. Climatol.* **2011**, *31*, 200–217.

10. Tran, H.; Uchihama, D.; Ochi, S.; Yasuoka, Y. Assessment with satellite data of the urban heat island effects in Asian mega cities. *Int. J. Appl. Earth Obs. Geoinform.* **2006**, *8*, 34–48.

11. Cui, Y.Y.; de Foy, B. Seasonal variations of the urban heat island at the surface and the near-surface and reductions due to urban vegetation in Mexico City. *J. Appl. Meteorol. Climatol.* **2012**, *51*, 855–868.

12. Li, X.; Zhou, W.; Ouyang, Z.; Xu, W.; Zheng, H. Spatial pattern of greenspace affects land surface temperature: evidence from the heavily urbanized Beijing metropolitan area, China. *Landsc. Ecol.* **2012**, *27*, 887–898.

13. Elsayed, I.S.M. Effects of population density and land management on the intensity of urban heat islands: A case study on the city of Kuala Lumpur, Malaysia. In *Application of Geographic Information Systems*; InTech: London, UK, 2012.

14. Zhou, B.; Diego, R.; Jürgen, P.K. The role of city size and urban form in the surface urban heat island. *Sci. Rep.* **2017**, *7*, 4791.

15. Solecki, W.D.; Rosenzweig, C.; Parshall, L.; Pope, G.; Clark, M.; Cox, J.; Wiencke, M. Mitigation of the heat island effect in urban New Jersey. *Global Environ. Chang. part B Environ. Hazards* **2005**, *6*, 39–49.

16. Oke, T.R. City size and the urban heat island. *Atmos. Environ.* **1973**, *7*, 769–779.

17. Howard, L. *The Climate of London, Deduced from Meteorological Observations, Made at Different Places in the Neighbourhood of the Metropolis*; W. Phillips: London, UK, 1818; Volume 2, pp. 1818–1820.

18. Oke, T.R. The Heat Island of the Urban Boundary Layer: Characteristics, Causes and Effects. In *Wind climate in cities*; Cermak, J.E., Davenport, A.G., Plate, E.J., Viegas, D.X., Eds.; Springer: Dordrecht, The Netherlands, 1995; pp. 81–107.

19. Voogt, J.A.; Oke, T.R. Thermal remote sensing of urban climates. *Remote Sens. Environ.* **2003**, *86*, 370–384.

20. Akbari, H.; Pomerantz, M.; Taha, H. Cool surfaces and shade trees to reduce energy use and improve air quality in urban areas. *Sol. Energy* **2001**, *70*, 295–310.

21. Wong, N.H.; Yu, C. Study of green areas and urban heat island in a tropical city. *Habitat Int.* **2005**, *29*, 547–558.

22. Bowler, D.E.; Buyung-Ali, L.; Knight, T.M.; Pullin, A.S. Urban greening to cool towns and cities: A systematic review of the empirical evidence. *Landsc. Urban Plan.* **2010**, *97*, 147–155.

23. Bonan, G.B. Effects of land use on the climate of the United States. *Clim. Chang.* **1997**, *37*, 449–486.

24. Hamada, S.; Ohta, T. Seasonal variations in the cooling effect of urban green areas on surrounding urban areas. *Urban For. Urban Green.* **2010**, *9*, 15–24.

25. Chen, A.; Yao, X.A.; Sun, R.; Chen, L. Effect of urban green patterns on surface urban cool islands and its seasonal variations. *Urban For. Urban Green.* **2014**, *13*, 646–654.

26. Zhang, X.; Zhong, T.; Feng, X.; Wang, K. Estimation of the relationship between vegetation patches and urban land surface temperature with remote sensing. *Int. J. Remote Sens.* **2009**, *30*, 2105–2118.

27. Yu, C.; Hien, W.N. Thermal benefits of city parks. *Energy Build.* **2006**, *38*, 105–120.

28. Oliveira, S.; Andrade, H.; Vaz, T. The cooling effect of green spaces as a contribution to the mitigation of urban heat: A case study in Lisbon. *Build. Environ.* **2011**, *46*, 2186–2194.

29. Kantzioura, A.; Kosmopoulos, P.; Zoras, S. Urban surface temperature and microclimate measurements in Thessaloniki. *Energy Build.* **2012**, *44*, 63–72.

30. Li, J.; Song, C.; Cao, L. Impacts of landscape structure on surface urban heat islands: A case study of Shanghai, China. *Remote Sens. Environ.* **2011**, *115*, 3249–3263.

31. Cao, X.; Onishi, A.; Chen, J.; Imura, H. Quantifying the cool island intensity of urban parks using ASTER and IKONOS data. *Landsc. Urban Plan.* **2010**, *96*, 224–231.

32. Lu, J.; Li, C.; Yang, Y.; Zhang, X.; Jin, M. Quantitative evaluation of urban park cool island factors in mountain city. *J. Cent. South Univ.* **2012**, *19*, 1657–1662.

33. Connors, J.P.; Galletti, C.S.; Chow, W.T.L. Landscape configuration and urban heat island effects: assessing the relationship between landscape characteristics and land surface temperature in Phoenix, Arizona. *Landsc. Ecol.* **2013**, *28*, 271–283.

34. Wong, N.H.; Jusuf, S.K.; Win, A.A.L.; Thu, H.K.; Negara, T.S. Environmental study of the impact of greenery in an institutional campus in the tropics. *Build. Environ.* **2007**, *42*, 2949–2970.

35. Jonsson, P. Vegetation as an urban climate control in the subtropical city of Gaborone. *Int. J. Climatol.* **2004**, *24*, 1307–1322.

36. Turner, M.G. Landscape ecology: What is the state of the science? *Ann. Rev. Ecol. Evol. Sens.* **2005**, *36*, 319–344.

37. Gustafson, E.J. Quantifying landscape spatial pattern: What is the state of the art? *Ecosystems* **1998**, *1*, 143–156.

38. Zhibin, R.; Haifeng, Z.; Xingyuan, H.; Dan, Z.; Xingyang, Y. Estimation of the Relationship Between Urban Vegetation Configuration and Land Surface Temperature with Remote Sensing. *J. Indian Soc. Remote Sens.* **2015**, *43*, 89–100.

39. Maimaitiyiming, M.; Ghulam, A.; Tiyip, T.; Pla, F.; Latorre-Carmona, P.; Halik, Ü.; Caetano, M. Effects of green space spatial pattern on land surface temperature: Implications for sustainable urban planning and climate change adaptation. *ISPRS J. Photogramm. Remote Sens.* **2014**, *89*, 59–66.

40. Zhou, W.; Huang, G.; Cadenasso, M.L. Does spatial configuration matter? Understanding the effects of land cover pattern on land surface temperature in urban landscapes. *Landsc. Urban Plan.* **2011**, *102*, 54–63.

41. Zhao, C.; Fu, G.; Liu, X.; Fu, F. Urban planning indicators, morphology and climate indicators: A case study for a north-south transect of Beijing, China. *Build. Environ.* **2011**, *46*, 1174–1183.

42. Chang, C.R.; Li, M.H.; Chang, S.D. A preliminary study on the local cool island intensity of Taipei city parks. *La ndsc. Urban Plan.* **2007**, *80*, 386–395.

43. Beijing Statistics Bureau. *Beijing Statistical Yearbook 2015*; China Statistics Press: Beijing, China, 2015.

44. Xia, X.A.; Chen, H.B.; Wang, P.C.; Zhang, W.X.; Goloub, P.; Chatenet, B.; Eck, T.F.; Holben, B.N. Variation of column-integrated aerosol properties in a Chinese urban region. *J. Geophys. Res. Atmos.* **2006**, *111*, doi:10.1029/2005JD006203.

45. Memon, G.R. Education in Pakistan: The key issues, problems and the new challenges. *J. Manag. Soc. Sci.* **2007**, *3*, 47–55.

46. Shah, M.H.; Nazia, S. Seasonal behaviours in elemental composition of atmospheric aerosols collected in Islamabad, Pakistan. *Atmos. Res.* **2010**, *95*, 210–223.

47. Jin, M.; Li, J.; Wang, J.; Shang, R. A practical split-windowalgorithmfor retrieving land surface temperature from Landsat-8 data and a case study of an urban area in China. *Remote Sens.* **2015**, *7*, 4371–4390.

48. Li, Z.L.; Tang, B.H.; Wu, H.; Ren, H.; Yan, G.; Wan, Z.; Trigo, I.F.; Sobrino, J.A. Satellite-derived land surface temperature: Current status and perspectives. *Remote Sens. Environ.* **2013**, *131*, 14–37.

49. Rozenstein, O.; Qin, Z.; Derimian, Y.; Karnieli, A. Derivation of land surface temperature for Landsat-8 TIRS using a split window algorithm. *Sensors* **2014**, *14*, 5768–5780.

50. Du, C.; Ren, H.Z.; Qin, Q.M.; Meng, J.J.; Li, J. Split-window algorithm For estimating land surface temperature from Landsat 8 TIRs data. In Proceedings of the 2014 IEEE International Geosciences and Remote Sensing Symposium, Quebec, QC, Canada, 13–18 July 2014.

51. Jimenez-Munoz, J.C.; Sobrino, J.A.; Skokovic, D.; Matter, C.; Cristobal, J. Land surface temperature retrieval methods fromLandsat-8 Thermal Infrared Sensor data. *IEEE Geosci. Remote Sens. Lett.* **2014**, *11*, 1840–1843.

52. Wang, F.; Qin, Z.; Song, C.; Tu, L.; Karnieli, A.; Zhao, S. An improved mono-window algorithm for land surface temperature retrieval from Landsat 8 thermal infrared sensor data. *Remote Sens.* **2015**, *7*, 4268–4289.

53. Qin, Z.; Karnieli, A.; Berliner, P. A mono-window algorithm for retrieving land surface temperature from Landsat TM data and its application to the Israel-Egypt border region. *Int. J. Remote Sens.* **2001**, *22*, 3719–3746.

54. Skokovic, D.; Sobrino, J.A.; Jimenez-Munoz, J.C.; Soria, G.; Julien, Y.; Mattar, C.; Cristobal, J. Calibration and Validation of Land Surface Temperature for Landsat 8—TIRS Sensor. In Proceedings of the Land product Validation and Evolution, Frascati, Italy, 28–30 January 2014.

55. Strehl, A.; Ghosh, J. Cluster ensembles—A knowledge reuse framework for combining partitionings. *J. Mach. Learn. Res.* **2002**, *3*, 93–99.

56. Pluim, J.P.W.; Maintz, J.B.A.; Viergever, M.A. Mutual-Information-Based Registration of Medical Images: A Survey. *IEEE Trans. Med. Imag.* **2003**, *22*, 986–1004.

57. Cover, T.; Thomas, J. *Elements of Information Theory*; Wiley-Interscience: Hoboken, NJ, USA, 1991.

58. Allaby, M. *A Dictionary of Earth Sciences,* 3rd ed.; Oxford University Press Inc.: New York, NY, USA, 2008; p. 460.

59. Press, W.H.; Teukolsky, S.A.; Vetterling, W.T.; Flannery, B.P. Section 14.7.3. Conditional Entropy and Mutual Information. In *Numerical Recipes: The Art of Scientific Computing*, 3rd ed.; Cambridge University Press: Cambridge, UK, 2007, ISBN 978-0-521-88068-8.

60. White, J.V.; Steingold, S.; Fournelle, C.G. Performance metrics for group-detection algorithms. In Proceedings of the 36th Symposium on the Interface, Baltimore, MD, USA, 26–29 May 2004.

61. Sridhar, D.V.; Bartlett, E.B.; Seagrave, R.C. Information theoretic subset selection for neural network models. *Comput. Chem. Eng.* **1998**, *22*, 613–626.

62. Press, W.H.; Flannery, B.P.; Teukolsky, S.A.; Vetterling, W.T. *Numerical Recipes*; Cambridge University Press: Cambridge, UK, 1990.

63. Strehl, A.; Ghosh, J. Cluster ensembles—A knowledge reuse framework for combining multiple partitions. *J. Mach. Learn. Res.* **2003**, *3*, 583–617.

64. Yang, Z.; Dong, J.; Liu, J.; Zhai, J.; Kuang, W.; Zhao, G.; Qin, Y. Accuracy Assessment and Inter-Comparison of Eight Medium Resolution Forest Products on the Loess Plateau, China. *ISPRS Int. J. Geo Inf.* **2017**, *6*, 152.

65. Tilahun, A.; Teferie, B. Accuracy assessment of land use land cover classification using google earth. *Am. J. Environ. Prot.* **2015**, *4*, 193–198.

66. McGarigal, K.; Cushman, S.A.; Neel M.C.; Ene, E. FRAGSTATS: Spatial Pattern Analysis Program for Categorical Maps, Computer Software Program Produced by the Authors at the University of Massachusetts. 2002. Available online: http://www.umass.edu/landeco/research/fragstats/fragstats.html (accessed on 6 August 2016).

67. Riva-Murray, K.; Riemann, R.; Murdoch, P.; Fischer, J.M.; Brightbill, R. Landscape characteristics affecting streams in urbanizing regions of the Delaware River Basin (New Jersey, New York, and Pennsylvania, US). *Landsc. Ecol.* **2010**, *25*, 1489–1503.

68. Du, H.; Cai, W.; Xu, Y.; Wang, Z.; Wang, Y.; Cai, Y. Quantifying the Cool Island Effects of Urban Green Spaces Using Remote Sensing Data. *Urban For. Urban Green.* **2017**, *27*, 24–31.

69. Yang, C.; He, X.; Wang, R.; Yan, F.; Yu, L.; Bu, K.; Zhang, S. The Effect of Urban Green Spaces on the Urban Thermal Environment and Its Seasonal Variations. *Forests* **2017**, *8*, 153–167.

70. Chen, X.L.; Zhao, H.M.; Li, P.X.; Yin, Z.Y. Remote sensing image-based analysis of the relationship between urban heat island and land use/cover changes. *Remote Sens. Environ.* **2006**, *104*, 133–146.

71. Huang, G.; Zhou, W.; Cadenasso, M.L. Is everyone hot in the city? Spatial pattern of land surface temperatures, land cover and neighborhood socioeconomic characteristics in Baltimore, MD. *J. Environ. Manage.* **2011**, *92*, 1753–1759.

72. Weng, Q.; Lu, D.; Schubring, J. Estimation of land surface temperature–vegetation abundance relationship for urban heat island studies. *Remote Sens. Environ.* **2004**, *89*, 467–483.

73. Kim, J.H.; Gu, D.; Sohn, W.; Kil, S.H.; Kim, H.; Lee, D.K. Neighborhood landscape spatial patterns and land surface temperature: An empirical study on single-family residential areas in Austin, Texas. *Int. J. Environ. Res. Pub. Health* **2016**, *13*, 880.

74. Kong, F.; Yin, H.; James, P.; Hutyra, L.R.; He, H.S. Effects of spatial pattern of greenspace on urban cooling in a large metropolitan area of eastern China. *Landsc. Urban Plan.* **2014**, *128*, 35–47.

75. Jin, M.S.; Kessomkiat, W.; Pereira, G. Satellite-Observed urbanization characters in Shanghai, China: Aerosols, urban heat island effect, and land-Atmosphere interactions. *Remote Sens.* **2011**, *3*, 83–99.

76. Jayalakshmy, M.S.; Philip, J. Thermophysical properties of plant leaves and their influence on the environment temperature. *Int. J. Thermophys.* **2010**, *31*, 2295–2304.

77. Notice of Beijing Municipal Bureau of Landscape and Forestry on Printing and Distributing the Work Plan of Urban Greening in 2016. Available online: http://www.bjyl.gov.cn/zwgk/fgwj/qtwj/201602/t20160202_176411.shtml (accessed on 14 September 2017).

78. 13th Five-Year, Landscape and Greening Plan of Beijing. Available online: http://news.xinhuanet.com/local/2016-01/06/c_128600299.htm (accessed on 14 September 2017).

79. Tong, H.; Liu, H.; Li, Y.; Sang, J.; Hu, F. Acyuality of summer urban heat island and the impact of urban planning wedge-shaped greenland to reducing the intensity of urban heat island in Beijing. *J. Appl. Meteorol. Sci.* **2005**, *16*, 257–266. (In Chinese)